Fast array analysis using a combination of FDTD and matrix manipulation techniques

V. Douvalis, Y. Hao and C.G. Parini

Abstract: In many cases, antenna array design and modelling are performed by the finite difference time domain (FDTD) method. The method is robust but very demanding in computer memory and CPU power. The authors present a new method that allows otherwise impractical FDTD simulations to produce valid results with no great dissipation of computer power. This is achieved with a combined effort of reduced full-wave simulations and matrix manipulations in the proposed array geometry. With the new scheme, the computational limitations of the conventional FDTD analysis are surpassed and the scope of the analysis itself is broadened; changes in electrical characteristics of an array, such as beam scanning, do not necessitate new simulation runs.

1 Introduction

Along with the increasing use of complex antenna arrays in broadband mobile communications and advanced radar systems, there have been intensive efforts in accurate prediction of array performance such as near-field distributions, far-field radiation patterns and mutual couplings [1]. For example, the method of moments (MoM) has been used to solve the integral equations pertaining to the mutual coupling effect [2]. However, the computational resources needed are proportional to some power of the number of unknowns and therefore it makes numerical simulation on medium size arrays impractical on a personal computer. In the FDTD algorithm, the problem remains, although the computational burden is only linearly proportional to the simulated space [3]. According to our knowledge, so far there have been very few attempts for implementing an efficient FDTD algorithm to analyse the medium sized arrays [4, 5]. In [4] a general method is presented using a basic reaction integral approach to achieve improvements in computer time of an order of magnitude for the case of a 5-element array. It is estimated that this improvement would be about two orders of magnitude for arrays of between 20–30 elements. Furthermore the method is only demonstrated for some specific antenna types (e.g. wire dipoles [4] and printed dipoles [5]).

In this paper we present a novel method for dramatically reducing the amount of computer resources needed for an FDTD analysis of antenna arrays. The purpose is to predict the electric and magnetic fields without resorting to a full wave simulation of the whole array structure but rather taking a small part of it into account. Radiating and scattering fields are computed from the single elements and then manipulated in accordance with the array geometry. The manipulations are performed by the use of matrix operations leading to a generalised array factor. Two study cases are presented: one with an array of conical horn antennas and the other with open-ended rectangular waveguides. All simulations are achieved by the conventional FDTD algorithms combined with a MATLAB™ code that provides the matrix manipulations and performed on a personal computer. Numerical results are compared with those from full FDTD simulations and the measurement data in good agreement.

IEE Proceedings online no. 20045078

doi:10.1049/ip-map:20045078

Paper first received 3rd August and in revised form 15th December 2004

The authors are with the Department of Electronic Engineering, University of London, Queen Mary, London E1 4NS, UK

E-mail: y.hao@elec.qmul.ac.uk

2 Methodology

2.1 Matrix formulation

The formulation is based on an element-by-element approach. It breaks up the array into constituent elements of which a small part will be modelled by the FDTD and then forms them as an entity again. This procedure can be reflected from a matrix representation, that is one global matrix $\{E\}_{global}$ to stand for near electric fields in the whole array, comprised of sub-matrices $\{E\}_k$ $(k = 1, 2 \ldots n)$ that represent the constituent elements as shown in (1):

$$\{E\}_{global} = \begin{bmatrix} \{E\}_1 & \{E\}_2 & \{E\}_3 \ldots & \\ & \bullet & & \\ & & \bullet & \\ & & & \{E\}_n \end{bmatrix} \quad (1)$$

It is understood from (1) that the position of an entry $(\{E\}_1, \{E\}_2 \ldots \{E\}_n)$ in the global matrix represents the spatial information of the near-field data (radiated or scattered fields) of the corresponding elements $(1, 2 \ldots n)$. Normally, the aforementioned data is extracted from a virtual surface located in the near field region of the array. This surface can always be placed in a uniform grid (since it is in the free space), making the notation in (1) applicable even when non-uniform grids are introduced to mesh the array itself. In general, the radiating near-field from a planar antenna array depends on two parameters: radiating fields of individual elements and scattering fields from their neighbours responsible for the mutual coupling. Thereby, two quantities are required in the array analysis:

$\vec{E}_{rad}$: radiating field from each element with the neglecting of mutual coupling;

$\vec{E}_{sc}$: scattering field owing to the presence of other elements.

Consequently, each sub-matrix in (1) will be the summation of radiating and scattering fields, hence:

$$\{E\}_i = \{E_{rad}\}_i + \{E_{sc}\}_i \tag{2}$$

Eventually, the global matrix $\{E\}_{global}$ consists of a global radiating matrix $\{E_{rad}\}_{global}$ and a global scattering matrix $\{E_{sc}\}_{global}$. It is clear that the global radiating matrix will be equal to $\{E_{rad}\}_1$ in the hypothetical situation of one-element array. However, if two elements are present in distance $\lambda \cdot \Delta$ (Δ is the uniform spatial grid increment measured on the virtual near-field surface and λ an integer), the global radiation matrix can be arranged as:

$$[E_{rad}]^2 = \begin{bmatrix} \{0\} & \{0\} & \cdots \{0\} & \{0\} \\ \{0\} & \{E_{rad}\}_1 & \cdots \{E_{rad}\}_2 & \{0\} \\ \{0\} & \{0\} & \cdots \{0\} & \{0\} \end{bmatrix} \tag{3}$$

$\lambda -$ columns

Since each grid point in the near-field surface has a one-to-one mapping in the global matrix, the separation distance of $\lambda \cdot \Delta$ between two antenna elements can be translated into λ columns in (3). Dimensions of the global matrix ($n \times n$) are determined by the span of the near-field area, which must be large enough for accurately predicting its far-field pattern.

2.2 Matrix manipulation

A single FDTD run of one stand-alone antenna element in free space can produce all the necessary radiation sub-matrices for the entire array. Let us consider a 5-element cross-shaped open-ended rectangular waveguide array depicted in Fig. 1. Only simulation of the central antenna element is needed and other sub-matrices for radiating fields can be derived from

$$abs(\{E_{rad}\}_i) = X_i \cdot abs(\{E_{rad}\}_1) \tag{4}$$

$$phase(\{E_{rad}\}_i) = phase(e^{j\theta_i} \cdot \{E_{rad}\}_1) \tag{5}$$

X_i is the power ratio of the feeds and θ_i is their phase difference. Both operators of *abs* and *phase* are applied to the individual elements of each sub-matrix. Once the radiating sub-matrices are obtained from the FDTD simulation, they will be placed inside the global matrix in line with the array topology. For example in this situation:

$$[E_{rad}]^5 = \left.\begin{bmatrix} \{0\} & \{E_{rad}\}_4 & \{0\} \\ \{E_{rad}\}_3 & \{E_{rad}\}_1 & \{E_{rad}\}_2 \\ \{0\} & \{E_{rad}\}_5 & \{0\} \end{bmatrix}\right\} \lambda - \text{rows} \tag{6}$$

$\lambda -$ columns

And the scattering matrix:

$$[E_{sc}]^5 = \left.\begin{bmatrix} \{0\} & \{E_{sc}\}_4 & \{0\} \\ \{E_{sc}\}_3 & \{E_{sc}\}_1 & \{E_{sc}\}_2 \\ \{0\} & \{E_{sc}\}_5 & \{0\} \end{bmatrix}\right\} \lambda - \text{rows} \tag{7}$$

$\lambda -$ columns

The procedure to obtain the scattering matrix in (7) is somewhat different from the procedure used for calculating the radiation matrix in (6). Whereas in (6) only one element (unit cell) simulation was enough to produce all the radiation sub-matrices, (7) can be obtained after the simulation of the field in the presence of a second element. The introduction of the second element, placed at the adjacent unit cell provides the scattering field information needed for (7). It has to remain inactive so that only its scattered field $\vec{E}_{sc}$ is added to the already calculated $\vec{E}_{rad}$ field of the radiating element. There are other issues involved in the construction of (7) that are going to be elucidated in the two case studies presented in the following Sections.

As a remark in the notation we specify that the sub-matrix $\{E_{sc}\}_j$ represents scattered fields owing to radiations from the jth element; $\{E_{rad}\}_i$ stands for radiation fields from the ith element. Also, the global matrices $[E_{rad}]^i$ and $[E_{sc}]^i$ will be identified by the superscript i that denotes the number of elements in the array.

In (6), $\{E_{rad}\}_2$ is placed in such a position, so as to represent the distance in physical space between the elements 1 and 2 or equivalently the shifting of coordinates: $(x,\ y) \rightarrow (x + \lambda \cdot \Delta,\ y)$. Since the global matrices represent the physical space of antenna arrays, the corresponding operation to the shifting of coordinates in the matrices is to reallocate the columns by λ places to the right. We denote the operator/matrix to perform the above function as S_n and its properties are indicated in the Appendix. Accordingly S_{-n} shifts the columns of a matrix, n places to the left. With the help of the aforementioned operators we can establish other radiation sub-matrices from $[E_{rad}]_1$: $[E_{rad}]_2 = [E_{rad}]_1 \cdot [S]_n$ and similarly for the third element $[E_{rad}]_3 = [E_{rad}]_1 \cdot [S]_{-n}$.

In addition, when two antenna elements in the array have the same radiation characteristics then the scattered fields at the antenna 1 owing to the radiation of antenna 2 $C_{1\rightarrow 2}$, is symmetrical to those at the antenna 2 owing to the radiation of the antenna 1, $C_{2\rightarrow 1}$. Hence, such a property of imaging symmetry can be denoted as a matrix $[O]_{x,y}$ (details of its definition can be found in the Appendix). It should be noted that the symmetry matrices do not alter the operating mode characteristics when the mode is symmetrical but it will introduce a 180° phase shift when it is anti-symmetrical. Therefore the scattering parameters must follow this change accordingly. Of course if the radiation characteristics of two antennas differ in amplitude and phase, (4) and (5) are applicable to the scattered fields as well.

Figure 2 shows simulated results of the 5-element array (Fig. 1) by using the proposed matrix manipulation technique and the full FDTD method, respectively. It can

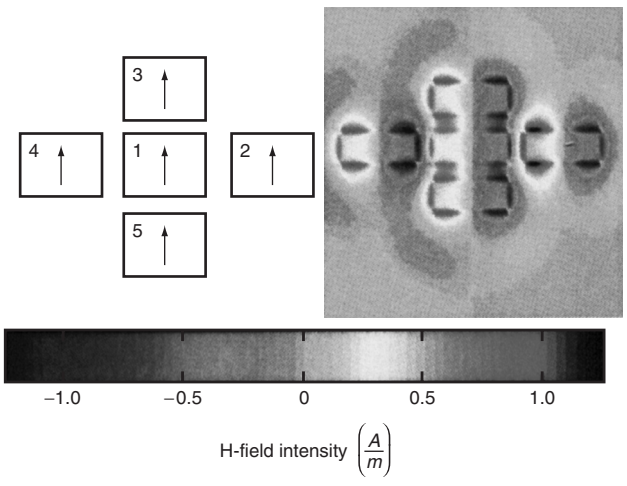

Fig. 1 *Field snapshot of 5-element array with open-ended rectangular waveguides*

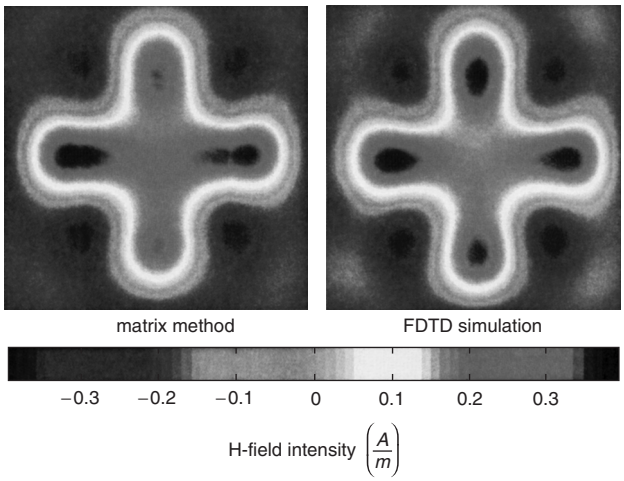

Fig. 2 *Comparison of magnetic field intensity (for array shown in Fig. 1) obtained from full FDTD and proposed matrix manipulation technique*

be seen that the near-field snapshots obtained from both methods agree with each other very well. However, the full FDTD approach requires the computation of all the antenna elements and it becomes impractical when the antenna array size increases. On the contrary, in the matrix manipulation method, a reduced FDTD programme was used to calculate only the radiation of one open-ended waveguide and its interaction with two neighbouring elements. The whole array behaviour is then calculated with the help of aforementioned operators in the matrix manipulation. Its efficiency can be further evident from two case studies in the following Section.

3 Two case studies

3.1 Conical horn antenna array

The first example is a conical horn antenna array fed by circular waveguides and excited in the TE_{11} mode. It is a part of a 7-element cluster. The central element is excited in phase with and 10.5 dB above the 6 surrounding elements (Fig. 3). By inspection, the interaction between elements 1 and 2 and that between 1 and 4 should provide all the necessary information needed for modelling scattering fields in the antenna array under an assumption that:

- Only the scattering from the closest elements is considered;
- Only the coupling effect produced by the central element is taken into account.

The above conditions are based on the fact that the surrounding elements radiate 10.5 dB below the central one. Apart from the radiation of element 1 alone (Fig. 4*c*), the matrix method records the interaction of the elements 1 and 2 (Fig. 4*a*) and that of elements 1 and 4 (Fig. 4*b*). In all three cases it is worth noting that only element 1 is radiating

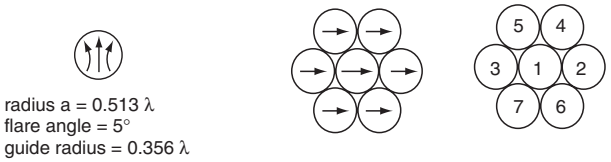

Fig. 3 *Prototype of conical horn antenna array and its dimensions*

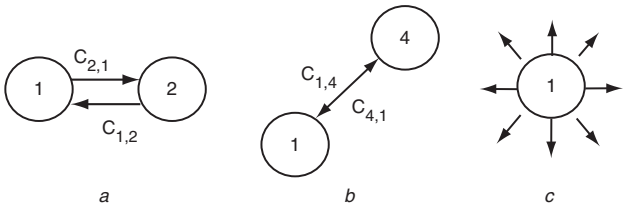

Fig. 4 *Illustration of matrix manipulation method in conical horn antenna array modelling*
a Interaction of elements 1 and 2
b Interaction of elements 1 and 4
c Radiation of element 1

while the others remain inactive. The purpose of these simulations is:

(i) To account for radiations of all the 7 elements: from the local distorted nonorthogonal FDTD simulation [6] on the element shown in Fig. 4*c*, radiation fields are computed and denoted as $[E_{rad}]_1 \cdot e^{j\cdot\theta_1}$. Therefore radiation fields from the other 6 elements can be obtained as $[E_{rad}]_k \cdot e^{j\cdot\theta_k}$, $k = 2, 3 \ldots 7$, where $[E_{rad}]_k = [E_{rad}]_1 - 10.5\,\text{dB}$ and $\theta_k = \theta_1$.

(ii) To account for the coupling between the central element and all the other elements: for calculating mutual couplings between the central element and its neighbours, $C_{1,3}$ and $C_{1,5}$ will be viewed as the mirror images through the vertical axis of $C_{1,2}$ and $C_{1,4}$; $C_{1,6}$ and $C_{1,7}$ are the mirror images through the horizontal axis of $C_{1,4}$ and $C_{1,5}$, respectively. Therefore, the only couplings that have to be computed are corresponding to the scattering sub-matrix denoted as $C_{1,2}$, yielding $[E_{sc}]^2_{1\to2}$ and $C_{1,4}$, yielding the sub-matrix $[E_{sc}]^2_{1\to4}$. Finally we obtain the global scattering matrix as:

$$[E_{sc}]^7_1 = [E_{sc}]^2_{1\to2} + [E_{sc}]^2_{1\to3} + [E_{sc}]^2_{1\to4} + [E_{sc}]^2_{1\to5} + [E_{sc}]^2_{1\to6} + [E_{sc}]^2_{1\to7} \quad (8)$$

where,

$$[E_{sc}]^2_{1\to3} = [E_{sc}]^2_{1\to2} \cdot [O]_y \quad (9)$$

$$[E_{sc}]^2_{1\to5} = [E_{sc}]^2_{1\to4} \cdot [O]_y \quad (10)$$

$$[E_{sc}]^2_{1\to6} = [E_{sc}]^2_{1\to4} \cdot [O]_x \quad (11)$$

$$[E_{sc}]^2_{1\to7} = [E_{sc}]^2_{1\to5} \cdot [O]_x \quad (12)$$

Now that both the radiation and coupling effects have been calculated as sub-matrices, we can gather them into one radiation and one scattering global matrix (Figs. 5 and 6). The total field is then:

$$[E_{total}] = [E_{rad}]^7 + [E_{sc.}]^7 \quad (13)$$

$$[H_{total}] = [H_{rad}]^7 + [H_{sc.}]^7 \quad (14)$$

Equations (13) and (14) contain all the data needed for the near-to-far field algorithm. Figure 7 shows the comparison of the conical horn antenna array radiation patterns obtained from the measurement [7], the full FDTD and the proposed matrix manipulation technique. All results show very good agreement. In Table 1, the computer resources needed by the FDTD and the matrix manipulation method are listed. The difference between two approaches is expected to increase in favour of the matrix manipulation method in large size arrays. Moreover, changes in the array's electrical characteristics such as beam

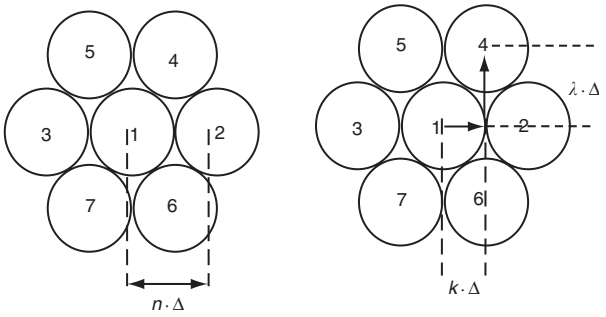

Fig. 5 *Configuration of conical horn antenna array*

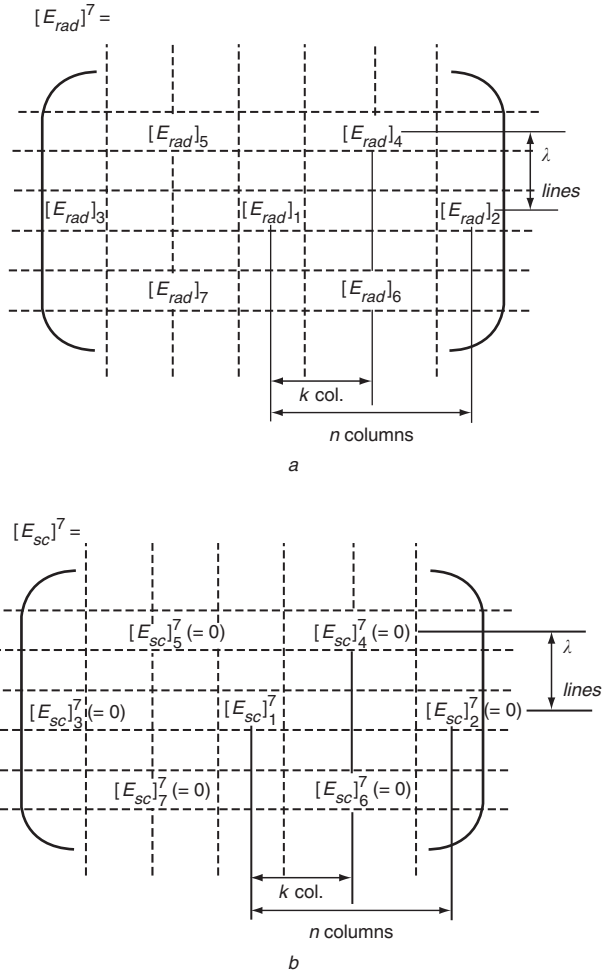

Fig. 6 *Matrix representation of elements in conical horn antenna array*

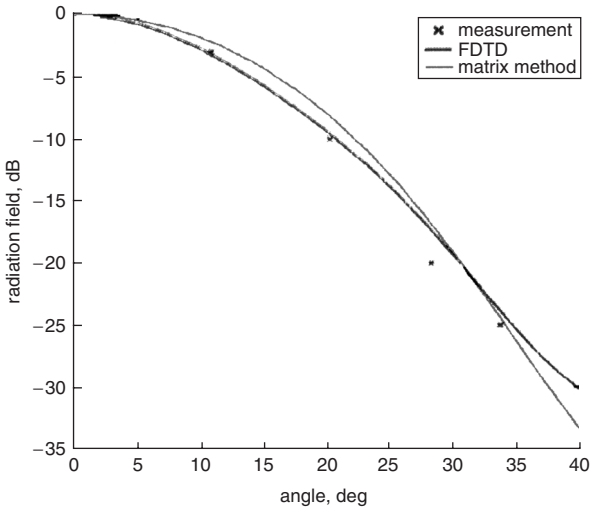

Fig. 7 *Comparison on radiation patterns of conical horn antenna array obtained from matrix manipulation, full FDTD and measurement*

Table 1: Computer resources used by full FDTD and matrix manipulation method

	Time (min)	Memory (Mbytes)	Time (min) to simulate the same array when changes occur (phase or power)
FDTD	16	370	16
MM	13	280	0

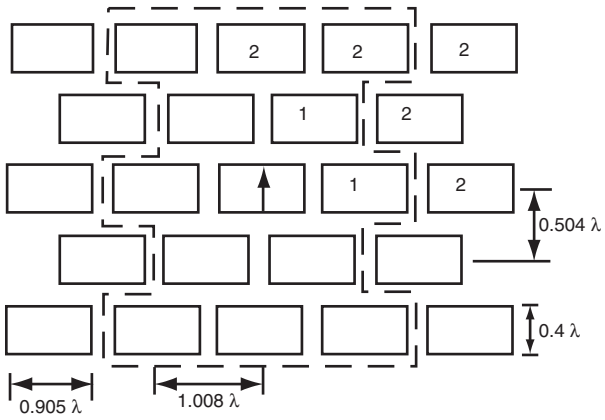

Fig. 8 *Prototype of Diamond's antenna array*

scanning do not necessitate new simulation runs in the matrix manipulation method.

3.2 Diamond's array

Here is studied an array of 23 elements presented by Diamond [8], in which only the central element is driven. An illustration is given in Fig. 8 along with the array dimensions. A full FDTD simulation is constrained by computer resources and hence only a reduced size array excluding the edge elements can be simulated. Since the array is very small compared to the operating wavelength, the edge diffraction components may well be significant and could cause distortions in the pattern shape. The matrix manipulation method however can be used to analyse the entire array without neglecting the edge elements. In this case, the second order mutual coupling (defined as coupling from elements marked as '2' in Fig. 8 in contrast to elements marked as '1' which denotes the first order mutual coupling) cannot be dismissed. Since only the central element is excited, the global radiating matrix $[E_{rad}]^{23}$ will be the same as $\{E_{rad}\}_1$. The global scattering matrix however will be more complicated. $[E_{sc}]_1^8$ accounts for the scattered field produced by the central element in the presence of the 7 neighbouring elements enumerated in Fig. 8 (upper right part of the array). By means of the matrix manipulations we can acquire the scattering upper left part of the array as mirror symmetry through the vertical axis:

$$[E_{sc}]_1^8 \cdot [O]_y \rightarrow \textit{upper left part} \qquad (15)$$

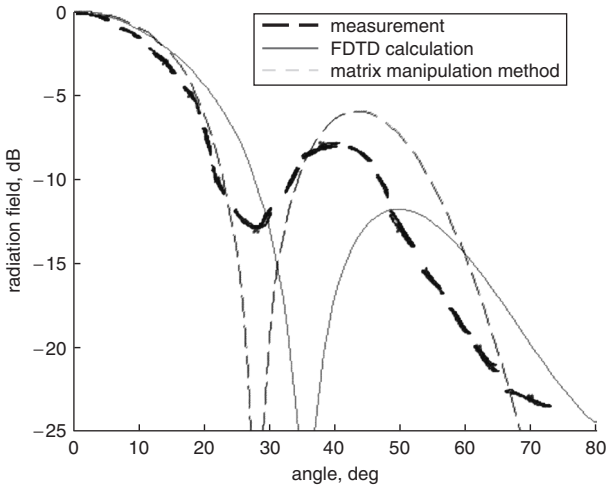

Fig. 9 *Comparison on radiation patterns of Diamond antenna array obtained from matrix manipulation, full FDTD and measurement*

By doing so, the summation of the two parts yields the complete scattering upper part:

$$[E_{sc}]_1^8 \cdot (I_n + [O]_y) \rightarrow \textit{upper part} \tag{16}$$

And the final step is to complete the array with the bottom part, which is the mirror image of the upper part through the horizontal axis:

$$[E_{sc}]_1^8 \cdot (I_n + [O]_y) \cdot [O]_x \rightarrow \textit{bottom part} \tag{17}$$

The resulting global scattering matrix can be summed up as:

$$[E_{sc}]_{global}^{23} = [E_{sc}]_1^8 \cdot (I_n + [O]_y) \cdot (I_n + [O]_x) \tag{18}$$

In Fig. 9, radiation patterns obtained from the full FDTD simulation on a truncated array and the proposed matrix manipulation method on the original array are compared with measured results [9]. It can be seen that the full FDTD simulation of the confined Diamond's array is not adequate. The exclusion of the edge elements results in the shift of the null in radiation pattern, while the measurements [9] indicate a local minimum at 35 degrees. However, the matrix manipulation method though has given a correct prediction in the position of the null and a more acceptable pattern shape (Fig. 9).

4 Conclusions

A combination of FDTD and matrix manipulation techniques has been proposed for fast analysis of medium size planar antenna arrays. Conventionally, a full FDTD simulation on such antenna arrays is very demanding in computer memory and CPU power. On some occasions, only confined models can be simulated and hence result in inaccurate results. The proposed matrix manipulation method has been demonstrated to reduce the computational

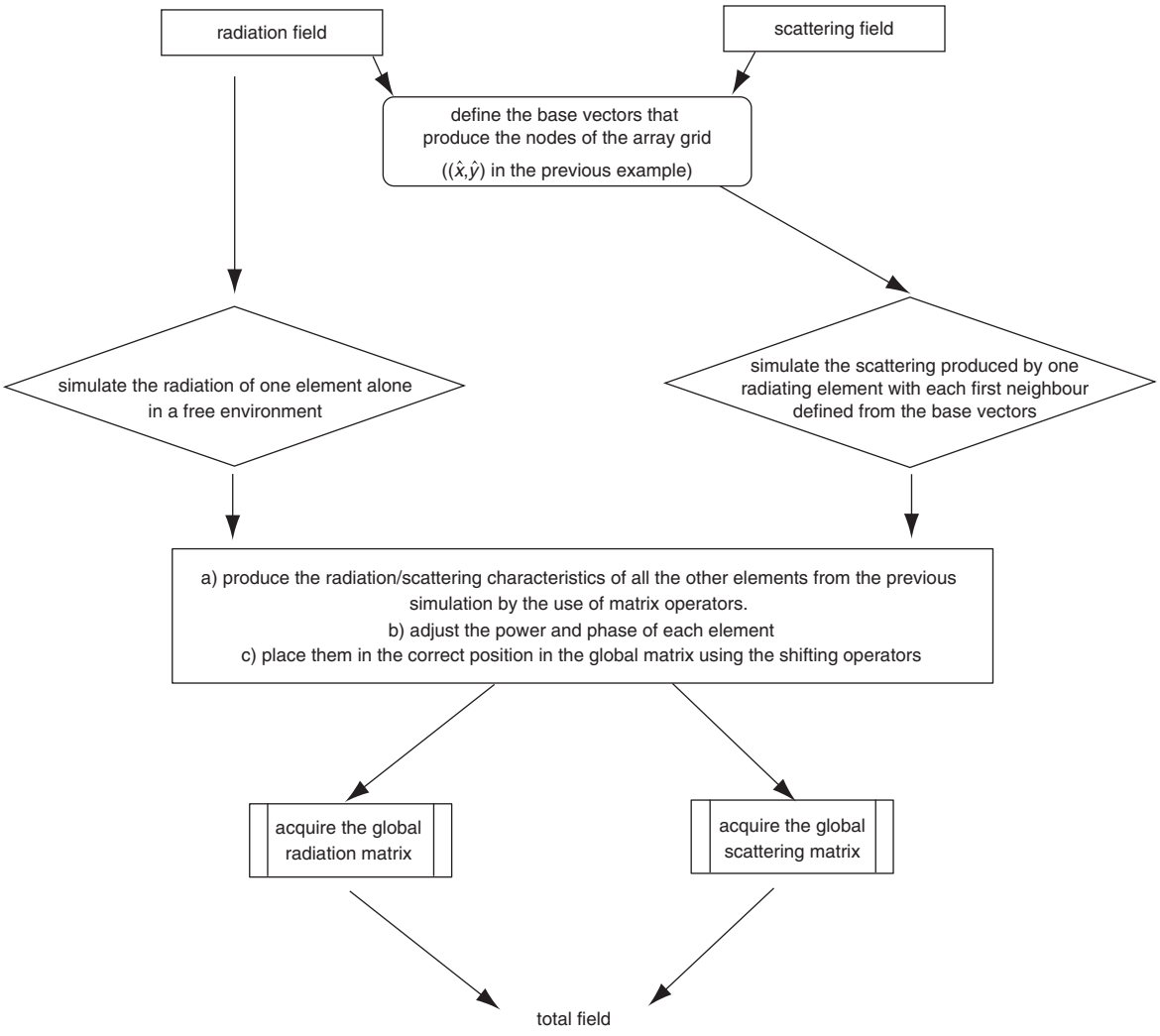

Fig. 10 *Flow chart illustrating matrix manipulation method*

efforts dramatically with the help of matrices/operators that utilise symmetrical properties of antenna elements in the array topology. The method has been validated by simulating a conical antenna array and a Diamond's array in good agreement with measurement results. A flow chart that sums up the method is given in Fig. 10. The method can lead to a group of generalised equations that can be applied to simulate not only medium size phased arrays, but also finite size periodic structures such as electromagnetic bandgap structures.

5 References

1 Amitay, N., Galindo, V., and Wu, C.P.: 'Theory and analysis of phased array antennas' (Wiley-Interscience, New York, 1972)
2 Sing, L.K., Chet, K.V., Djuanda, J.N., and Sze, L.T.: 'Analysis of slotted waveguide structure using MoM techniques'. NCTT 2003 Proc., Jan. 2003, pp. 40–44
3 Holter, H., and Steyskal, H.: 'On the size requirement for finite phased-array models', *IEEE Trans. Antennas Propag.*, 2002, **50**, pp. 836–840
4 Railton, C.J., Meade, S.A., and Hilton, G.S.: 'New methodology for the analysis of finite arrays of complex antenna elements', *Electron. Lett.*, 1996, **32**, pp. 784–785
5 Railton, C.J., and Hilton, G.S.: 'The analysis of medium-sized arrays of complex elements using a combination of FDTD and reaction matching', *IEEE Trans. Antennas Propag.*, 1999, **47**, pp. 707–714
6 Hao, Y., and Railton, C.J.: 'Analyzing electromagnetic structures with curved boundaries on Cartesian FDTD meshes', *IEEE Trans. Microw. Theory Tech.*, 1998, **46**, (1), pp. 82–88
7 Tun, S.M.: 'Array fed offset reflector antennas'. PhD thesis, Dept. of Electrical Engineering, Queen Mary College, University of London, 1984
8 Diamond, B.L.: 'Small arrays- their analysis and their use for design of array elements' in Oliner, and Knittel, (Eds.).: 'Phased array antennas' (Artech House, 1970)
9 Kitchener, D.: 'Mutual coupling in finite planar arrays of rectangular apertures'. PhD thesis, Dept. of Electrical Engineering, Queen Mary College, University of London, 1989

6 Appendix

In this Appendix, some details of matrix transformations are illustrated.

6.1 Shifting of the coordinates

6.1.1 Shifting to the right: It is the operation $(x, y) \rightarrow (x + n \cdot \Delta, y)$. Its equivalent transformation in the matrix space is to shift the original matrix n columns to the right. Such an operator is:

$$[S]_n = \begin{bmatrix} & & n-\text{columns} & & \\ & & \overbrace{} & & \\ & & & 0 & \\ & & \diagdown & & \\ & & 1 & & \\ & 0 & & & \\ & & & \diagdown & \end{bmatrix} \tag{19}$$

When it is multiplied from the left by a matrix of the same dimensions it produces the desired result:

$$[E_{rad}] = \begin{bmatrix} \{0\} & \{0\} & \{0\} \\ \{0\} & \{E\} & \{0\} \\ \{0\} & \{0\} & \{0\} \end{bmatrix} \cdot [S]_n = \begin{bmatrix} \{0\} & \{0\} & \cdots\{0\} & \{0\} \\ \{0\} & \{0\} & \cdots\{E\} & \{0\} \\ \{0\} & \{0\} & \cdots\{0\} & \{0\} \end{bmatrix} \quad \overbrace{\phantom{n-\text{columns}}}^{n-\text{columns}} \tag{20}$$

6.1.2 Shifting to the left: It is the operation $(x, y) \rightarrow (x - n \cdot \Delta, y)$. The matrix for this operation is denoted as $[S]_{-n}$:

$$[S]_{-n} = \begin{bmatrix} & & & \overbrace{\phantom{n\ \text{rows}}}^{n\ \text{rows}} & \\ & & & 0 & \\ & & \diagdown & & \\ & & 1 & & \\ & 0 & & & \\ & & & \diagdown & \end{bmatrix} \tag{21}$$

As that in 6.1.1:

$$[E_{rad}] = \begin{bmatrix} \{0\} & \{0\} & \{0\} \\ \{0\} & \{E\} & \{0\} \\ \{0\} & \{0\} & \{0\} \end{bmatrix} \cdot [S]_{-n} = \begin{bmatrix} \{0\} & \{0\}\cdots & \{0\} & \{0\} \\ \{0\} & \{E\}\cdots & \{0\} & \{0\} \\ \{0\} & \{0\}\cdots & \{0\} & \{0\} \end{bmatrix} \quad \overbrace{\phantom{n-\text{columns}}}^{n-\text{columns}} \tag{22}$$

6.1.3 Shifting upwards: It is the operation $(x, y) \rightarrow (x, y + n \cdot \Delta)$. The transformation matrix is the same as the one used in 6.1.1, but now multiplied from the left. If we denote it as $[U]_n$ we will have $[U]_n = [S]_n$ and

$$[E_{rad}] = [U]_n \cdot \begin{bmatrix} \{0\} & \{0\} & \{0\} \\ \{0\} & \{E\} & \{0\} \\ \{0\} & \{0\} & \{0\} \end{bmatrix} = \left.\begin{bmatrix} \{0\} & \{0\} & \{0\} \\ \{0\} & \{E\} & \{0\} \\ \vdots & \vdots & \vdots \\ \{0\} & \{0\} & \{0\} \\ \{0\} & \{0\} & \{0\} \end{bmatrix}\right\} \tag{23}$$

6.1.4 Shifting downwards: It is the operation $(x, y) \rightarrow (x, y - n \cdot \Delta)$. The transformation matrix is the same as the one used in 6.1.2. As that in 6.1.3, we will have $[U]_{-n} = [S]_{-n}$ and

$$[E_{rad}] = [U]_{-n} \cdot \begin{bmatrix} \{0\} & \{0\} & \{0\} \\ \{0\} & \{E\} & \{0\} \\ \{0\} & \{0\} & \{0\} \end{bmatrix} = \left.\begin{bmatrix} \{0\} & \{0\} & \{0\} \\ \{0\} & \{0\} & \{0\} \\ \vdots & \vdots & \vdots \\ \{0\} & \{E\} & \{0\} \\ \{0\} & \{0\} & \{0\} \end{bmatrix}\right\} \tag{24}$$

6.2 Mirror/reflection images

6.2.1 Reflection of the space in the y-axis: The matrix operator that produces the transformation $(x, y) \rightarrow (-x, y)$ is denoted as $[O]_y$:

$$[O]_y = \begin{bmatrix} 0 & 0 & 0 & & & 1 \\ 0 & 0 & 0 & & & 0 \\ 0 & 0 & 0 & & & 0 \\ 0 & 0 & 0 & . & . & 0 \\ 0 & 0 & 1 & & & 0 \\ 0 & 1 & 0 & & & 0 \\ 1 & 0 & 0 & & & 0 \end{bmatrix} \tag{25}$$

So if a matrix [E] consists of the columns $\{a\}_1$, $\{a\}_2 \ldots \{a\}_n$, then its reflected matrix will be:

$$[E] = \begin{bmatrix} \vdots & \vdots & \cdots & \vdots \\ \{a\}_1 & \{a\}_2 & \cdots & \{a\}_n \\ \vdots & \vdots & \cdots & \vdots \end{bmatrix} \cdot [O]_y = \begin{bmatrix} \vdots & \vdots & \cdots & \vdots \\ \{a\}_n & \{a\}_{n-1} & \cdots & \{a\}_1 \\ \vdots & \vdots & \cdots & \vdots \end{bmatrix} \quad (26)$$

6.2.2 Reflection of the space in the x-axis: The matrix will be the same as the previous one but now it must multiply from the left. So if a matrix [E] consists of the lines $\{a\}_1$, $\{a\}_2 \ldots \{a\}_n$ then the $(x, y) \rightarrow (x, -y)$ is represented by: $[O]_x = [O]_y$ and

$$[E] = [O]_x \cdot \begin{bmatrix} \cdots & \{a\}_1 & \cdots \\ \cdots & \{a\}_2 & \cdots \\ \vdots & \vdots & \vdots \\ \cdots & \{a\}_n & \cdots \end{bmatrix} = \begin{bmatrix} \cdots & \{a\}_n & \cdots \\ \cdots & \{a\}_{n-1} & \cdots \\ \vdots & \vdots & \vdots \\ \cdots & \{a\}_1 & \cdots \end{bmatrix} \quad (27)$$